THE JOURNAL OF PHYSICAL CHEMISTRY B

ARTICLE

pubs.acs.org/JPCB

Formation of Ag Nanoparticle-Doped Foam-like Polymer Films at the Liquid−Liquid Interface

Li Lin,[†] Ke Shang,[†] Xingtao Xu,[†] Chunxiao Chu,[†] Huihui Ma,[†] Yong-Ill Lee,[‡] Jingcheng Hao,[†] and Hong-Guo Liu*[,†]

[†]Key Laboratory for Colloid and Interface Chemistry of Education Ministry, Shandong University, Jinan 250100, P. R. China

[‡]Anastro Laboratory, Department of Chemistry, Changwon National University, Changwon 641-773, Republic of Korea

ABSTRACT: The composite poly(2-vinylpyridine) (P2VP)-Ag^+ foam-like thin films were prepared at the interface between $AgNO_3$ aqueous solution and polymer chloroform solution at 25 °C. An X-ray photoelectron spectroscopy (XPS) investigation indicated that Ag^+ ions in the composite films were partially transformed to Ag atoms after irradiated by UV-light and completely transformed to Ag atoms after being treated with KBH_4 aqueous solution. Ag nanoparticles with the average sizes of 2.71 ± 0.82 and 3.28 ± 1.20 nm were generated in these two transferred films with different treatments, respectively. Transmission electron microscopy (TEM) and high-resolution TEM (HRTEM) images showed clearly that the composite films were composed of microcapsules whose walls had multilayer structures, and the nanoparticles were incorporated in the walls. The formation of the composite films at the liquid−liquid interface was attributed to the adsorption of the polymer molecules at the interface, coordination between the pyridine groups and Ag^+ ions, and self-assembly of the composite molecules. Furthermore, the catalytic activity of the composite films was evaluated using the reduction of 4-nitrophenol (4-NP) by KBH_4. The results demonstrated that the composite thin films have high and durable catalytic activity.

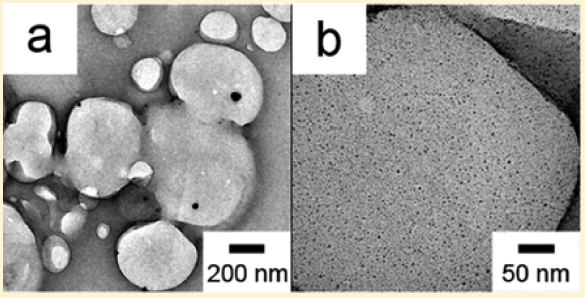

1. INTRODUCTION

Noble metal nanoparticles, including Au, Ag, Pt, and Pd, have attracted considerable interest owing to unique optical, electronic, and catalytic properties. It was demonstrated that the catalytic activity of metal nanoparticles was increased with decreasing the particle size in heterogeneous catalytic systems because of the increase of the specific surface area and chemical potential of the particles.[1,2] Hence, the facile synthesis of novel metal nanoparticles with small sizes is a very important task in both the feverishly evolving disciplines of nanotechnology and thin film preparation methodologies. The nanoparticles are usually embedded in or adsorbed on matrices such as metal oxides[3−5] and carbon-based materials[6−8] when they are used as catalysts. Recently, researchers have found that novel metal nanoparticles embedded in or adsorbed on polymer matrices exhibited higher catalytic activities.[2] These include the incorporation of metal nanoparticles in polymer films,[9] polymer microgels,[10−12] and polymer nanofibers[13] for catalytic investigations.

Polymer microcapsules possess a high surface area, a large cavity, and porous walls. So they can encapsulate active species, protect them from environmental hazards, and release them selectively. Besides the selective permeability for different species, the polymer microcapsules have good mechanical properties, and their solubility in different solvents can be easily tuned by modifying the outermost layer.[14,15] These properties make them have wide applications in a variety of research fields in science and technology. Several approaches have been proposed to prepare polymer microcapsules.[16,17] When metal nanoparticles are adsorbed on or embedded in the capsule walls, they would exhibit high catalytic activities due to the large surface area of the capsules, the high loading of the nanoparticles, and the porous walls that allow free diffusion of the reactants and products. For these reasons, many efforts have been devoted to the preparation of polymer capsule composite nanostructures functionalized with metal nanoparticles in recent years.

Generally, the preformed microcapsule adsorbed metal precursors at first and then metal nanoparticles were formed and attached on the outer surface,[18] outer and inner surfaces,[19] or embedded in the walls of the capsules through the reduction process of metal ions.[20] Metal nanoparticles can also be incorporated into the walls by depositing polyelectrolyte and preformed colloid particles alternatively[21] or by adsorbing and reducing the metal precursors during the layer-by-layer deposition process.[22] In addition, metal nanoparticles could also be attached on the inner surface of the microcapsules by depositing polymer layers and then removing the templates after the formation of metal nanoparticles on the template surface.[23] Polymer microcapsules doped with Au, Ag, and Pd nanoparticles were prepared though these procedures, and their optical[18,21] and catalytic properties[19,22,24] were explored.

Received: June 24, 2011
Revised: August 21, 2011
Published: August 24, 2011

ACS Publications © 2011 American Chemical Society

Scheme 1. Illustration of the Experimental Process: (a) Chloroform Solution of P2VP Filled in a Beaker; (b) a Clear Liquid−Liquid Interface Formed after Adding Aqueous Solution of $AgNO_3$; (c) a Thin Film Appeared at the Interface after a Certain Time

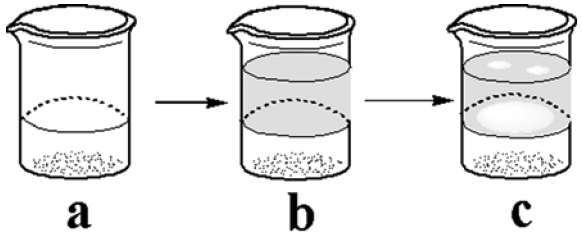

In our recent work, a new and facile method has been developed to prepare metal precursor-doped polymer microcapsules and thin foam-like films at the liquid−liquid interface. We found that foam-like films composed of microcapsules appeared at the liquid/liquid interface between a chloroform solution of P2VP and an aqueous solution of $HAuCl_4$ at room temperature after standing for several hours. After transferred onto solid substrates and irradiated using UV-light, homogeneous Au nanoparticles were generated with adsorbed on and embedded in the walls.[25] In this paper, this novel method was extended to prepare Ag nanoparticle-doped P2VP foam-like films. The size of the Ag nanoparticles was around 3 nm and exhibited high and durable catalytic activity for the reduction of 4-NP by KBH_4. The method described here is more simple, convenient, and cost-effective compared with the reported methods in the literature.

2. EXPERIMENTAL SECTION

2.1. Chemicals and Materials. Poly(2-vinylpyridine) (P2VP, M_w: 5300, M_n: 5000) was purchased from Sigma-Aldrich (St. Louis, MO, USA). $AgNO_3$ (>99.8%) was purchased from Shanghai Chem. Co. Chloroform (≥99.0%) obtained from Tianjin Guangcheng Chem. Co. is an analytical reagent containing 0.3−1.0% ethanol as a stabilizer. The water used herein was highly purified to a resistivity ≥18.0 MΩ cm. KBH_4 (≥97.0%) was purchased from Shanghai Zhanyun Chem. Co., Ltd. 4-Nitrophenol (4-NP) (analytical reagent) was obtained from Tianjin Guangfu Fine Chemical Research Institute.

2.2. Preparation and Characterization. Foam-like thin polymer films doped with Ag^+ ions were prepared at the liquid−liquid interface, as illustrated in Scheme 1. A 10 mL chloroform solution of P2VP with the concentration of 0.2 $mg \cdot mL^{-1}$ was poured in a beaker, and then a 10 mL aqueous solution of $AgNO_3$ with the concentration of 1×10^{-2} $mol \cdot L^{-1}$ was added carefully. A clear liquid−liquid interface was formed; the upper phase and lower phase were aqueous and organic solutions, respectively, due to the different densities of water and chloroform. Then the beaker was placed in a sealed container that was set in a dark oven. The temperature was controlled to be 25 °C. A thin film appeared at the liquid−liquid interface after 24 h. The film was transferred onto carbon-coated copper grids, silicon, and quartz slides for further treatment and characterization.

To reduce the doped Ag^+ ions to Ag atoms and to cause cross-linking of the polymer molecules,[26,27] the transferred films were irradiated by UV light with the wavelength of 254 nm directly.

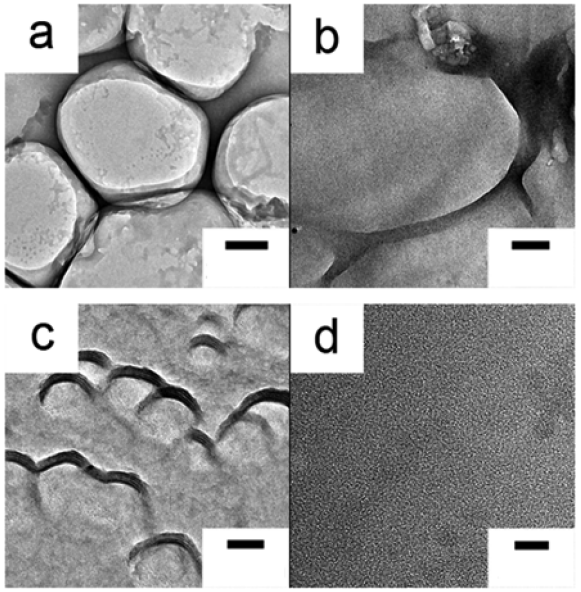

Figure 1. TEM micrographs of the composite P2VP−Ag^+ films formed at the liquid−liquid interface (scale = 200, 100, 100, and 20 nm for a, b, c, and d, respectively).

Otherwise, they were immersed in an aqueous solution of KBH_4 with the concentration of 1×10^{-4} $mol \cdot L^{-1}$ for 10 min and then irradiated by UV light. The power of the lamp was 6 mW, the distance between the lamp and the sample was tuned to be 15 cm, and the irradiation time was 1 h.

The morphology and structure of these samples were characterized by using high-resolution transmission electron microscopy (HRTEM, JEOL-2010) with an accelerating voltage of 200 kV. The compositions of these samples were probed by using X-ray photoelectron spectroscopy (XPS, ESCALAB MKII) with an Mg Kα ($h\nu$ = 1253.6 eV) exciting source at a pressure of 1.0×10^{-6} Pa and a resolution of 1.00 eV.

2.3. Catalytic Reaction. 4-NP aqueous solution (0.5 mL) with a concentration of 2×10^{-4} $mol \cdot L^{-1}$ was poured into a 1 cm quartz cuvette and 1.0 mL of a 2×10^{-2} $mol \cdot L^{-1}$ aqueous solution of KBH_4 was added, to produce final 4-NP and KBH_4 concentrations of 6.67×10^{-5} and 1.33×10^{-2} $mol \cdot L^{-1}$, respectively. The thin films deposited on quartz slides with pretreatment of KBH_4 solution and UV-light irradiation were immersed in the reaction system to catalyze the reduction of 4-NP. The reaction was monitored using UV−vis spectroscopy (HP-8453E) at room temperature (~20 °C).

3. RESULTS AND DISCUSSION

3.1. Morphology and Structure. Figure 1 shows the TEM micrographs of the composite films formed at the liquid−liquid interface. The microcapsules with the size of about several hundreds of nanometers appeared (Figure 1a,b) and contacted with one another to construct a foam-like structure. As can be seen from Figure 1c, the walls of some smaller microcapsules exhibited layered structures composed of 4−5 layers. However, it was difficult to find silver nanoclusters or nanoparticles in these samples, even in the high-magnification TEM image (Figure 1d). It implied that the Ag^+ ion was not reduced at the liquid−liquid interface during the film formation process.

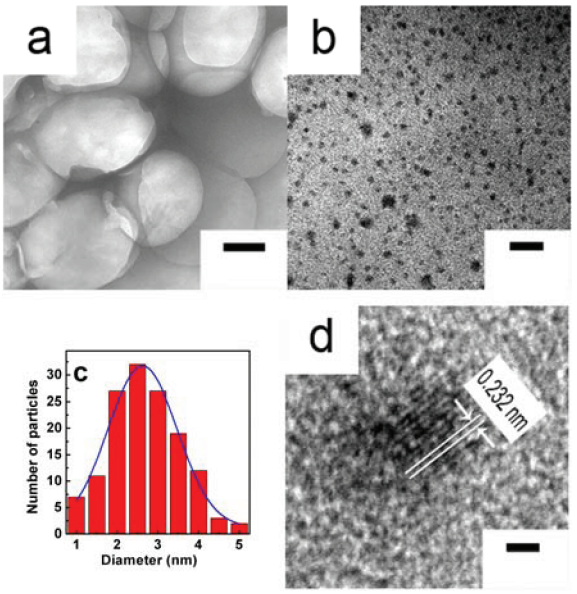

Figure 2. TEM (a,b) and HRTEM (d) images of the composite film after UV-light irradiation (scale = 300, 20, and 1 nm for a, b, and d, respectively). The size distribution histogram of the particles in b is shown in c.

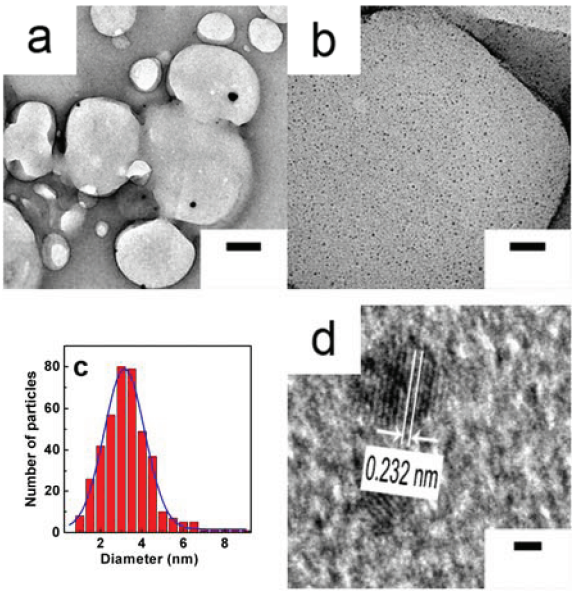

Figure 3. TEM (a,b) and HRTEM (d) images of the composite film after KBH_4 aqueous solution treatment and UV-light irradiation (scale = 200, 50, and 1 nm for a, b, and d, respectively). The size distribution histogram of particles in image b is shown in c.

A further process to reduce the Ag^+ ions to get Ag nanoparticles and induce the cross-linking of the polymer molecules to enhance the mechanical stability and antisolubility was carried out by irradiating the transferred films with UV light. Figure 2 shows the TEM and HRTEM micrographs and the particle size distribution histogram of the UV-light irradiated films. Ag nanoparticles were generated and distributed well in the film with preserving the foam-like structures, as clearly seen in Figure 2b. The average diameter of the particles was measured

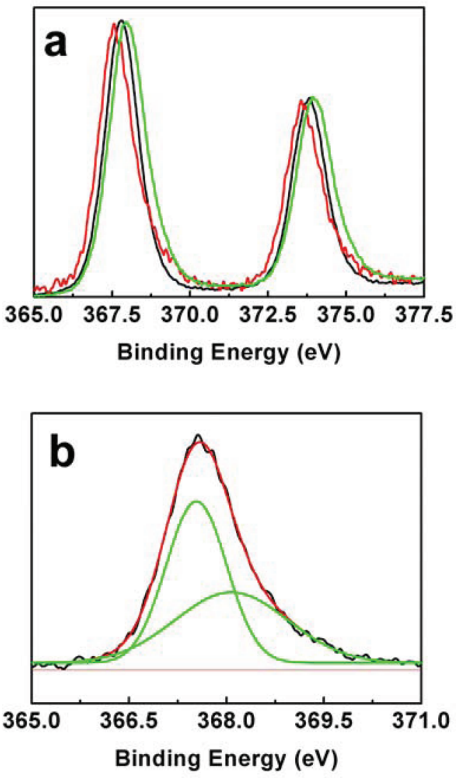

Figure 4. (A) Normalized XPS spectra of the composite films: as prepared (black), after UV-light irradiation (red), and after KBH_4 aqueous solution treatment and UV-light irradiation (green); (B) decomposition of the $Ag3d_{5/2}$ band in the composite film after UV-light irradiation by using Gaussian multipeak fitting.

to be 2.71 ± 0.82 nm. The HRTEM image gave clear lattice fringes. The distance between the adjacent fringes was estimated to be 0.232 nm, closing to the interplanar distance of (111) faces of Ag with a face-centered cubic (fcc) structure. This confirmed the formation of Ag nanoparticles. It would be expected that these films have good catalytic properties due to the small size of the nanoparticles and homogeneous distribution of the particles in the walls.

Figure 3 illustrates the TEM and HRTEM micrographs and particle size distribution histogram of the sample that was treated with aqueous solution of KBH_4 and then irradiated by UV light. It can be seen that well-distributed nanoparticles were generated in the wall along with preserving the foam-like structure and the layered wall. The average size of the particles was found to be 3.28 ± 1.20 nm, slightly greater than that of the particles in Figure 2b. In addition, the interplanar distance shown in the HRTEM image (Figure 3d) was measured to be 0.232 nm, indicating the formation of Ag nanoparticles.

3.2. Composition Analysis. The existence of silver element in the composite structures was also confirmed by means of X-ray photoelectron spectroscopy (XPS) shown in Figure 4. Two bands appeared around 368 and 374 eV in each curve, which correspond to $3d_{5/2}$ and $3d_{3/2}$ of silver, respectively. It should be noticed that the position and symmetry of the bands in the three curves are different from one another. The location of the XPS peaks of silver depends on the chemical states of silver element and the size of the particles.[28,29] The binding energies of 368.0−368.3, 367.6−367.8, and 367.3−367.4 eV were attributed

to $3d_{5/2}$ of Ag(0), Ag(I), and Ag(II), respectively.[30,31] Two symmetric bands centered at 367.8 and 373.8 eV were observed in the transferred film prepared without any treatment and assigned to $3d_{5/2}$ and $3d_{3/2}$ of Ag(I), respectively, as evidence of Ag^+ ions in this film. This result shows a good agreement with the TEM observation. Similarly, two symmetric bands appeared in the transferred film with KBH_4 treatment and UV-light irradiation, indicating that only one silver species exists in the film. Compared with the sample without any treatment, the position of the bands was shifted to 368.0 and 374.0 eV and assigned to $3d_{5/2}$ and $3d_{3/2}$ of Ag(0), respectively. This revealed that the Ag^+ ions were transformed to Ag atoms completely.

However, there are two differences in the case of UV-light irradiated films without KBH_4 treatment compared with the films without any treatments, that is, the shift of peak position to lower binding energy and an appearance of shoulder at higher binding energy area. The bands are also asymmetric, suggesting the existence of more than one kind of silver species. The $3d_{5/2}$ band could be well-resolved into two peaks centered at 367.6 and 368.1 eV with the relative amounts of 54.9 and 45.1%, respectively, by the Gaussian multipeak fitting method (Figure 4b). According to the literatures,[30,31] these peaks should be attributed to $3d_{5/2}$ of Ag(I) and Ag(0), respectively. This indicated that Ag^+ ions and Ag atoms coexisted in the film after UV-light irradiation. This result revealed that Ag^+ ions were transformed to Ag atoms incompletely and Ag^+ ions and Ag atoms coexisted in the film only after UV-light irradiation. This may be the reason why the size of the particles generated only by UV-light irradiation is less than that of the particles generated by KBH_4 treatment. Compared with the samples without any treatments, the peak corresponding to $3d_{5/2}$ of Ag(I) shifted slightly from 367.8 to 367.6 eV after UV-light irradiation. This may be related to the slight variation of the microenvironment around Ag^+ ions in these samples. Nevertheless, both of the peaks can be assigned to $3d_{5/2}$ of Ag(I) according to the literature.[30,31]

3.3. Formation Mechanism. P2VP is a kind of amphiphilic molecule to a certain extent. It can be dissolved in both water and organic solvents because the pyridine group has hydrophilicity and methylene units in polymer backbone are hydrophobic. When the liquid−liquid interface was formed, P2VP molecules moved to and were adsorbed onto the interface to reduce the interfacial free energy between two liquid phases. The hydrophilic pyridine group faced to the water phase and then coordinated with Ag^+ ions, while the methylene units faced the organic phase. Consequently, the thin film layer was formed in the interface by connecting P2VP chains with one another mediated by Ag^+ ions which could combine two pyridine groups. Several layers were gradually formed and overlapped with time, leading to the formation of a multilayer film at last.

The formation of the monolayer or multilayer thin films should be ascribed to the rapid adsorption of P2VP molecules at the liquid−liquid interface due to the interaction between Ag^+ ions and the pyridine groups. It was tried to use pure water instead of aqueous solutions of $AgNO_3$ or $HAuCl_4$ to prepare pure P2VP foam-like film at the liquid−liquid interface. However, no film appeared at the liquid−liquid interface, only some structures with different morphologies other than microcapsules appeared at the air−water interface, and the morphologies depended on the pH values of the water phase. This indicated that P2VP molecules transferred from the organic phase to the water phase gradually and adsorbed at the air−water interface at last in these cases. Because no special interaction existed between the polymer molecules and the species in the water phase, the adsorption speed of P2VP molecules at the liquid−liquid interface was very low. Once the polymer molecules were adsorbed at the interface, they entered the water phase rapidly, so no thin layer forms. When the aqueous solution of $AgNO_3$ with a lower concentration, such as 1×10^{-4} mol·L^{-1} was used, it was also difficult to form foam-like film at the liquid−liquid interface. Although there existed special interaction between Ag^+ ions and the polymer molecules, the adsorption speed of P2VP molecules at the liquid−liquid interface was still lower due to the low concentration of Ag^+. When the concentration of Ag^+ increased to 1×10^{-2} mol·L^{-1}, foam-like films formed at the liquid−liquid interface, and some thicker flat films were observed in some places. The adsorption of P2VP at the liquid−liquid interface was fast enough in this case. Large numbers of polymer molecules came together at the interface in a short time and organized into monolayer or/and multilayer thin films. This indicated that the formation of a thin flat film at the liquid−liquid interface should be a prerequisite for the formation of microcapsules and foam-like films at the liquid−liquid interface.

The thin multilayer film would also be amphiphilic to some extent. It is possible that its hydrophilicity is slightly stronger than its hydrophobicity due to the adsorption of Ag^+ ions and the stronger interaction between the ions and the species in the water phase, such as electrostatic interaction and hydration. So it inclined to enter the water phase. However, it would not be favorable from the viewpoint of energy if it entered into the water phase in the form of a thin flat film because the hydrophobic face of the film would come in contact with water to form a high-energy

Scheme 2. Schematic Presentation of the Formation Process of the Foam-like Thin Film at the Liquid−Liquid Interface: (a) Formation of the Liquid−Liquid Interface; (b) Adsorption of P2VP Molecules and Coordination of Pyridine Groups with Silver Ions; (c) Formation of a Monolayer; (d) Formation of a Multilayer; (e) Self-Assembly of the Multilayer to a Microcapsule; (f) Formation of a Foam-like Film via Congregation of the Microcapsules

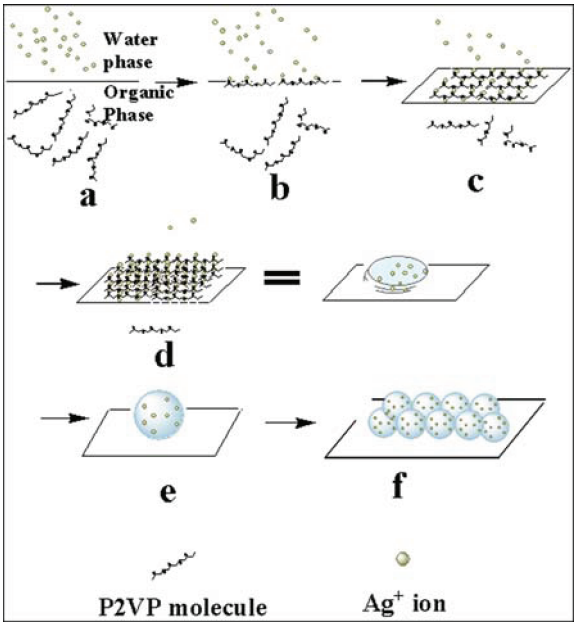

interface. Therefore, the film protruded, curled, and self-organized into a capsule whose outer surface was hydrophilic. More and more capsules formed with time and eventually congregated at the interface to form a foam-like film. Then how did the flat film further organized into a microcapsule? This would be attributed to the interfacial tension between the liquid and the film edge. It is reasonable to suppose that the formed flat films are round ones. Besides the interfacial tensions between the film and the water and organic phases, there would be an interfacial tension between the liquid and the film edge, which created an additional pressure directing to center of the film to cause the film to buckle in such a way that a capsule formed with the hydrophilic portion of the film on its external surface. If the film is too thicker, the film is too rigid to buckle. So only these films with appropriate thickness could self-assemble into microcapsules. This process was similar to the formation of poly(9-vinylcarbazole) nanotubes at the air−water interface.[32] The schematic illustration of the formation process is shown in Scheme 2.

Similar to the $HAuCl_4$ aqueous solution/P2VP chloroform solution system,[25] thin foam-like films and microcapsules also appeared at the air−water interface in this case. This further confirmed the proposed formation mechanism. Some microcapsules escaped from the liquid−liquid interface and entered the water phase due to their hydrophilic outer surfaces and then were captured by the air−water interface.

This is similar to the self-assembly process of P2VP at the liquid−liquid interface formed by chloroform solution of P2VP with an aqueous solution of $HAuCl_4$.[25] However, there are two obvious differences between them. First of all, the interactions between the polymer molecules and the inorganic species are different. At the liquid−liquid interface of P2VP chloroform solution and $HAuCl_4$ aqueous solution, the adsorbed P2VP molecules were protonated first because the water phase is highly acidic. Then the protonated pyridine groups attracted the gold complex anions to form composite thin films and then self-assembled into microcapsules, while the pyridine groups at the P2VP chloroform solution/$AgNO_3$ aqueous solution interface were coordinated with Ag^+ ions to form thin films and microcapsules. It should be remarked that pH values of the aqueous phases do not have significant influences on the formation of the composite Ag−P2VP microcapsules and foam-like films. The key factor for the formation of these nanostructures at the liquid−liquid interface is the strong interaction between P2VP molecules and the inorganic species in the water phase which leads to rapid adsorption of the polymer molecules at the interface. Second, the metal ions in two different systems show dissimilar behaviors during the film formation process. As discussed in our previous papers, $AuCl_4^-$ ions were partially reduced to Au atoms during the foam-like film formation process at the interface because the small amount of ethanol (about 0.2% (v/v)) was used as a reductant. However, Ag^+ ions were hardly reduced to atoms during this process. This should be attributed to different redox potentials of these ions. $AuCl_4^-$ ions are easier to be reduced than Ag^+ ions due to the higher redox potential.

3.4. Catalytic Properties. The reduction of 4-NP by $NaBH_4$ or KBH_4 has been widely used to evaluate the catalytic activities of noble metal nanoparticles.[3,9,12,33−35] We also adopted this reaction to investigate the catalytic performance of the Ag nanoparticle-doped P2VP foam-like thin films here. Figure 5a presents the successive UV−vis spectra of 4-NP aqueous solutions in the reaction system depending on various reaction times in the presence of the catalyst for the first catalytic cycle. The

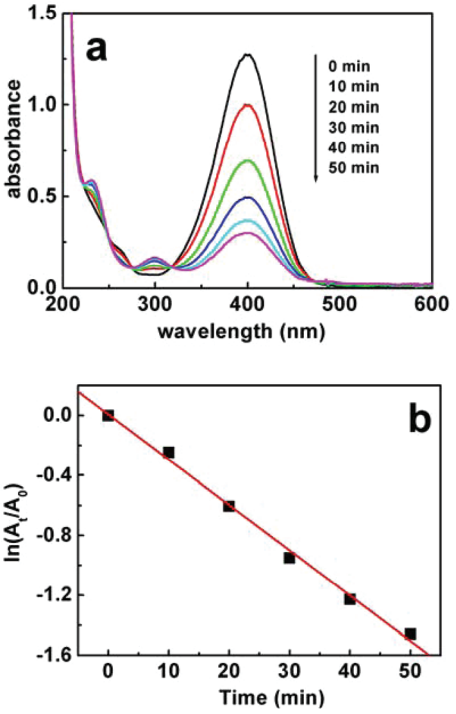

Figure 5. Time-dependent UV−vis spectra of the aqueous solution of 4-NP and KBH_4 in the presence of the composite film (a) and the relationship between $\ln(A_t/A_0)$ and t (b).

progress of the reaction was followed from the successive decrease of the absorption peak at 400 nm caused by phenolate ions in 4-NP, while a new peak at 300 nm appeared and increased gradually due to the formation of the corresponding amino compound, 4-aminophenol (4-AP). It is good evidence for the reduction of 4-NP by KBH_4 in the presence of the composite catalyst. The presence of isosbestic points also indicates that only 4-AP was produced from the catalytic reduction of 4-NP.[3,33,35]

The concentration of KBH_4 was much greater than that of 4-NP, so the reduction rate was assumed to be independent of the KBH_4 concentration and only dependent on the concentration of 4-NP. According to the Beer−Lambert law, the absorbance of 4-NP at $t = 0$ (A_0) and time t (A_t) should correspond to the concentrations at $t = 0$ (C_0) and time t (C_t), respectively, indicating that the ratio C_t/C_0 is equal to the ratio A_t/A_0. Figure 5b illustrates the relationship between $\ln(A_t/A_0)$ and reaction time. The linear relation between these two variables designates that the catalytic reduction of 4-NP followed pseudofirst-order rate kinetics with respect to 4-NP concentration. The apparent rate constant for the reduction of 4-NP by the composite catalyst was calculated to be 0.030 min^{-1} from the slope of the fit line for the first cycle. The composite thin film was used as a catalyst for several runs. The apparent rate constants for the second, the third, and the fourth cycles were found to be 0.027, 0.025, and 0.025 min^{-1}, respectively. This composite film exhibited high and durable catalytic activity. The higher catalytic activity should be attributed to the special structure of the composite thin film. The composite thin film has two apparent features. The first is the homogeneously embedded Ag nanoparticles with a small size which ensures the efficient specific surface area for the catalytic reaction. The second is the porous and foam-like structure of the polymer film which allows free

diffusion of the reactant and product. Although the Au nanoparticle-doped P2VP foam-like thin films exhibited much higher catalytic activity for the first cycle than that of Ag nanoparticle-doped one due to the higher loading of nanoparticles, their catalytic activities decreased rapidly in the second cycle because the size of Au nanoparticles increased due to aggregation and fusion.[25] On the contrary, the Ag nanoparticle-doped foamlike polymer film has good catalytic durability. This should be associated with the stability of Ag nanoparticles in the catalytic reaction systems. On the other hand, Ag is much cheaper than Au. So Ag−P2VP foam-like film can be used as an efficient and durable catalyst, which is cost-effective and easily prepared.

4. CONCLUSIONS

New Ag-nanoparticle doped foam-like P2VP films have been prepared through the coordination of polymer molecules with Ag^+ ions, the self-assembly of the composite molecules at the liquid−liquid interface, and subsequent reduction of Ag^+ ions by KBH_4 after transferred on solid substrates. Ag nanoparticles with the average diameter of 3.28 nm were embedded homogeneously in the walls. This is a facile and convenient way to prepare metal nanoparticle−polymer composites. The developed composite structure exhibited high and stable catalytic activity for the reduction of 4-NP in KBH_4 medium.

AUTHOR INFORMATION

Corresponding Author

*Tel.: 86-531-88362805. Fax: 86-531-88564750. E-mail: hgliu@sdu.edu.cn.

ACKNOWLEDGMENT

This work is supported by the National Natural Science Foundation of China (No. 20873078 and 21033005) and the National Basic Research Program of China (973 Program, No. 2009CB930103).

REFERENCES

(1) Haruta, M. *Chem. Rev.* **2003**, *3*, 75–87.
(2) Ishida, T.; Haruta, M. *Angew. Chem., Int. Ed.* **2007**, *46*, 7154–7156.
(3) Huang, X.; Guo, C.; Zuo, J.; Zheng, N.; Stucky, G. D. *Small* **2009**, *5*, 361–365.
(4) Pastoriza-Santos, I.; Perez-Juste, J.; Carregal-Romero, S.; Herves, P.; Liz-Marzan, L. M. *Chem. Asian J.* **2006**, *1*, 730–736.
(5) Pino, L.; Recupero, V.; Beninati, S.; Shukla, A. K.; Hegde, M. S.; Bera, P. *Appl. Catal., A* **2002**, *225*, 63–75.
(6) Ishida, T.; Kinoshita, N.; Okatsu, H.; Akita, T.; Takei, T.; Haruta, M. *Angew. Chem., Int. Ed.* **2008**, *47*, 9265–9268.
(7) Zheng, T.; Nishiyama, N.; Egashira, Y.; Ueyama, K. *Colloids Surf., A* **2005**, *262*, 52–56.
(8) Sanles-Sobrido, M.; Correa-Duarte, M. A.; Carregal-Romero, S.; Rodriguez-Gonzalez, B.; Alvarez-Puebla, R. A.; Herves, P.; Liz-Marzan, L. M. *Chem. Mater.* **2009**, *21*, 1531–1535.
(9) Hariprasad, E.; Radhakrishnan, T. P. *Chem.—Eur. J.* **2010**, *16*, 14378–14384.
(10) Biffis, A.; Minati, L. *J. Catal.* **2005**, *236*, 405–409.
(11) Biffis, A.; Cunial, S.; Spontoni, P.; Prati, L. *J. Catal.* **2007**, *251*, 1–6.
(12) Yang, H.; Nagai, K.; Abe, T.; Homma, H.; Norimatsu, T.; Ramaraj, R. *ACS Appl. Mater. Interfaces* **2009**, *1*, 1860–1864.
(13) Guo, S.; Dong, S.; Wang, E. *Small* **2009**, *5*, 1869–1876.
(14) Antipov, A. A.; Sukhorukov, G. B. *Adv. Colloid Interface Sci.* **2004**, *111*, 49–61.
(15) Peyratout, C. S.; Dhne, L. *Angew. Chem., Int. Ed.* **2004**, *43*, 3762–3783.
(16) Caruso, F. *Chem.—Eur. J.* **2000**, *6*, 413–419.
(17) Meier, W. *Chem. Soc. Rev.* **2000**, *29*, 295–303.
(18) Koo, H. Y.; Choi, W. S.; Kim, D.-Y. *Small* **2008**, *4*, 742–745.
(19) Han, J.; Liu, Y.; Guo, R. *Adv. Funct. Mater.* **2009**, *19*, 1112–1117.
(20) Kozlovskaya, V.; Kharlampieva, E.; Chang, S.; Muhlbauer, R.; Tsukruk, V. V. *Chem. Mater.* **2009**, *21*, 2158–2167.
(21) Skirtach, A. G.; Karageorgiev, P.; Bedard, M. F.; Sukhorukov, G. B.; Mohwald, H. *J. Am. Chem. Soc.* **2008**, *130*, 11572–11573.
(22) Antipov, A. A.; Sukhorukov, G. B.; Fedutik, Y. A.; Hartmann, J.; Giersig, M.; Mohwald, H. *Langmuir* **2002**, *18*, 6687–6693.
(23) Chen, Z.; Gang, T.; Zhang, K.; Zhang, J.; Chen, X.; Sun, Z.; Yang, B. *Colloids Surf., A* **2006**, *272*, 151–156.
(24) Wen, F.; Zhang, W.; Wei, G.; Wang, Y.; Zhang, J.; Zhang, M.; Shi, L. *Chem. Mater.* **2008**, *20*, 2144–2150.
(25) Chen, L.-J.; Ma, H.; Chen, K.-C.; Cha, H.-Y.; Lee, Y.-I.; Qian, D.-J.; Hao, J.; Liu, H.-G. *J. Colloid Interface Sci.* **2011**, *362*, 81–88.
(26) Li, X.; Zhao, S.; Zhang, S.; Kim, D. H.; Knoll, W. *Langmuir* **2007**, *23*, 6883–6888.
(27) Doycheva, M.; Stamenova, R.; Tsvetanov, Ch. B.; Adler, H. J. P.; Kuckling, D. *Macromol. Mater. Eng.* **2001**, *286*, 151–155.
(28) Lopez-Salido, I.; Lim, D. C.; Kim, Y. D *Surf. Sci.* **2005**, *588*, 6–18.
(29) Luo, K.; St. Clair, T. P.; Goodman, D. W. *J. Phys. Chem. B* **2000**, *104*, 3050–3057.
(30) Weaver, J. F.; Hoflund, G. B. *J. Phys. Chem.* **1994**, *98*, 8519–8524.
(31) Tjeng, L. H.; Meinders, M. B. J.; van Elp, J.; Ghijsen, J.; Sawatzky, G. A. *Phys. Rev. B* **1990**, *41*, 3190–3198.
(32) Wang, C.-W.; Xin, G.-Q.; Lee, Y.-I.; Hao, J.; Jiang, J.; Liu, H.-G. *J. Appl. Polym. Sci.* **2010**, *116*, 252–257.
(33) Kundu, S.; Wang, K.; Liang, H. *J. Phys. Chem. C* **2009**, *113*, 5157–5163.
(34) Murugadoss, A.; Chattopadhyay, A. *J. Phys. Chem. C* **2008**, *112*, 11265–11271.
(35) Saha, S.; Pal, A.; Kundu, S.; Basu, S.; Pal, T. *Langmuir* **2010**, *26*, 2885–2893.